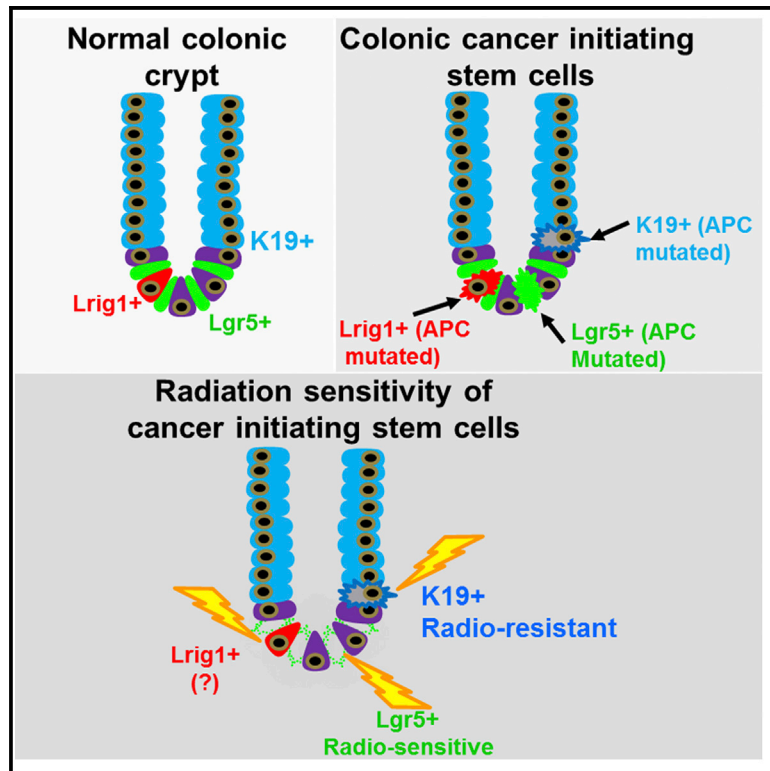# Cell Stem Cell

Krt19⁺/Lgr5⁻ Cells Are Radioresistant Cancer-Initiating Stem Cells in the Colon and Intestine

Graphical Abstract

Authors

Samuel Asfaha, Yoku Hayakawa, ..., Anil K. Rustgi, Timothy C. Wang

Correspondence

tcw21@columbia.edu

In Brief

Genetic-inducible fate-mapping studies suggest that intestinal epithelial cells are replaced from at least two principal stem cell pools. Asfaha et al. now identify Krt19⁺ cells in the colon that are long-lived, radioresistant cancer-initiating stem cells distinct from the previously described radiosensitive Lgr5⁺ stem cells.

Highlights

- *Krt19* marks long-lived colonic and intestinal stem cells above the crypt base

- *Krt19* stem cells render *Lgr5⁺* CBCs dispensable in colon and intestine

- Radioresistant *Krt19⁺* cancer-initiating cells are distinct from *Lgr5⁺* cells

- *Lgr5⁺* cancer stem cells are dispensable in *Krt19⁺* cell-derived APC floxed tumors

CrossMark

CellPress

Article

Krt19⁺/Lgr5⁻ Cells Are Radioresistant Cancer-Initiating Stem Cells in the Colon and Intestine

Samuel Asfaha,[1,7] Yoku Hayakawa,[1] Ashlesha Muley,[1] Sarah Stokes,[1] Trevor A. Graham,[3] Russell E. Ericksen,[1] Christoph B. Westphalen,[1] Johannes von Burstin,[5] Teresa L. Mastracci,[4] Daniel L. Worthley,[1] Chandhan Guha,[6] Michael Quante,[5] Anil K. Rustgi,[2] and Timothy C. Wang[1,*]

[1]Division of Digestive and Liver Diseases, Department of Medicine, Irving Cancer Research Center, Columbia University, New York, NY 10032, USA
[2]Division of Gastroenterology, Department of Medicine, Abramson Cancer Center, University of Pennsylvania, Philadelphia, PA 19104, USA
[3]Centre for Tumour Biology, Barts Cancer Institute, London EC1M 6BQ, UK
[4]Department of Genetics and Development, Columbia University, New York, NY 10032, USA
[5]II. Medizinische Klinik, Klinikum rechts der Isar, Technische Universität München, 81675 Munich, Germany
[6]Department of Radiation Oncology, Albert Einstein College of Medicine, New York, NY 10467, USA
[7]Department of Medicine, University of Western Ontario, London, ON N6A 5W9, Canada
*Correspondence: tcw21@columbia.edu
http://dx.doi.org/10.1016/j.stem.2015.04.013

SUMMARY

Epithelium of the colon and intestine are renewed every 3 days. In the intestine there are at least two principal stem cell pools. The first contains rapid cycling crypt-based columnar (CBC) *Lgr5⁺* cells, and the second is composed of slower cycling *Bmi1*-expressing cells at the +4 position above the crypt base. In the colon, however, the identification of *Lgr5⁻* stem cell pools has proven more challenging. Here, we demonstrate that the intermediate filament *keratin*-19 (*Krt19*) marks long-lived, radiation-resistant cells above the crypt base that generate *Lgr5⁺* CBCs in the colon and intestine. In colorectal cancer models, *Krt19⁺* cancer-initiating cells are also radioresistant, while *Lgr5⁺* stem cells are radiosensitive. Moreover, *Lgr5⁺* stem cells are dispensable in both the normal and neoplastic colonic epithelium, as ablation of *Lgr5⁺* stem cells results in their regeneration from *Krt19*-expressing cells. Thus, *Krt19⁺* stem cells are a discrete target relevant for cancer therapy.

INTRODUCTION

Adult tissue stem cells are characterized by multipotentiality and the capacity to self-renew (Li and Clevers, 2010). In the mouse small intestine and colon, the simple columnar epithelium is rapidly renewed every 3 days. Genetic-inducible fate-mapping studies suggest that epithelial cells in the small intestine are replaced from at least two principal stem cell pools, comprising both rapidly cycling crypt-based columnar (CBC) *Lgr5*-expressing cells and slower cycling *Bmi1*-expressing stem cells situated at position +4 above the crypt base (Barker et al., 2007;

Sangiorgi and Capecchi, 2008). In the small intestine, the stem cell markers *Sox-9* and *Hes1* are also expressed in actively cycling *Lgr5⁺* cells, while *Bmi*-1, *mTert, Hopx*, and *Lrig1* are expressed in relatively quiescent stem cells, confirming the existence of more than one stem cell pool (Fre et al., 2011; Furuyama et al., 2011; Montgomery et al., 2011; Powell et al., 2012; Takeda et al., 2011). Moreover, *Lgr5⁺* cells are dispensable in the small intestine, with *Bmi1⁺* stem cells able to regenerate *Lgr5⁺* cells and their lineages (Tian et al., 2011).

The epithelial lining of the colon is also comprised of a single layer of columnar epithelial cells, which are constantly renewed by a pool of committed stem cells. These colonic stem cells give rise to progeny that terminally differentiate into a number of lineages that include colonocytes, mucus-secreting goblet cells, and enteroendocrine cells. Most recent studies have suggested that colonic stem cells are located at the crypt base throughout the colon, and a number of markers for colon stem cells have been proposed, including Lgr5 (Barker et al., 2007), Lrig1 (Powell et al., 2012), Sox9 (Ramalingam et al., 2012), and EphB2 (Jung et al., 2011). Lgr5 has been the best studied, with in vivo lineage tracing showing that Lgr5-expressing cells at the colonic crypt base are capable of self-renewal and able to differentiate into all three colonic lineages. In the colon, however, it has been more challenging to identify the stem cells that reside above the crypt base. *Bmi1⁺* cells, for example, do not exist in the colon. Thus, it is not known whether more than one distinct stem cell pool exists in the colon.

Tumors are postulated to arise from tissue stem or progenitor cells, but the relative contribution of different stem cell pools to tumorigenesis remains unknown (Barker et al., 2009). In addition, our current understanding of colon cancer is based on a model of clonal evolution, whereby early adenomas advance to invasive carcinomas through stepwise acquisition of mutations (Fearon and Vogelstein, 1990). In rapidly proliferating tissues, such as the intestine or colon, however, this model of tumorigenesis implies that only stem cells are sufficiently long-lived to accumulate the requisite mutations. Indeed, the contribution of *Lgr5⁺*

stem cells to intestinal tumorigenesis has been demonstrated by the formation of adenomas upon targeted mutation of the *Apc* gene specifically in *Lgr5*^{+} cells (Barker et al., 2009). Nonetheless, the contribution of additional *Lgr5*-negative stem cells to the cellular origin of both colonic and intestinal cancer has not been clarified.

To determine if an *Lgr5*-negative stem cell contributes to colonic homeostasis and tumor initiation, we established a genetic fate-mapping system for labeling *keratin*-19 (*Krt19*)-expressing progenitor/stem cells. Cytokeratins are a multigene family of intermediate filaments, critical in the maintenance of the cytoskeleton but expressed in different lineages within the epithelium (Moll et al., 1982). Cytokeratin 19 or Krt19 is the smallest known acid keratin (∼40 kDa), is epithelial specific, and is found in a broad range of epithelial tissues. In the gastrointestinal tract, Krt19 expression is restricted to the proliferating compartments of the stomach, small intestine, and colon, as well as the pancreatic ducts of the adult pancreas and the hepatobiliary ducts (Brembeck et al., 2001). *Krt19* is expressed in the stem cell zone of the hair follicle (Brembeck et al., 2001; Lapouge et al., 2011; Means et al., 2008), is amplified in many solid tumors, and, as we demonstrate here, is expressed near the presumptive progenitor/stem cell zone of both the colon and intestine. More specifically, we examined *Krt19* because it is expressed at position +4, extending up to the isthmus, thus allowing us to selectively label a population of cells that includes transit-amplifying cells, progenitors, and long-lived stem cells, yet excludes rapidly cycling CBC *Lgr5*^{+} stem cells.

We compared *Krt19*^{+} cells above the crypt base to *Lgr5*^{+} CBC cells with respect to their response to epithelial injury and cancer-initiating ability. *Krt19*-expressing cells identify long-lived progenitors/stem cells distinct from *Lgr5*^{+} cells and additionally render *Lgr5*^{+} stem cells dispensable in both the colon and intestine. Under conditional loss of the *Apc* gene, *Krt19*^{+} stem cells also display cancer-initiating ability, yet are functionally distinct from *Lgr5*^{+} cancer-initiating cells by their relative radioresistance.

RESULTS

Krt19 Transcript Localizes to the Stem Cell Zone above the Crypt Base and Marks Both Colonic and Intestinal Stem Cells

To localize *Krt19* mRNA and protein expression, we performed in situ hybridization for *Krt19* mRNA and immunofluorescence staining for Krt19 protein. *Krt19* RNA was completely absent from the colonic crypt base and was detected primarily in the isthmus (i.e., area of crypt narrowing) that included cells extending down near the presumptive crypt progenitor/stem cell zone (Figure 1A; Figure S1A). In contrast, *Krt19* protein showed minimal overlap with *Krt19* RNA and was localized predominantly in differentiated cells (Figure S1B). Similarly, in the intestine, *Krt19* RNA was detected primarily in the isthmus, and not in the intestinal crypt base (Figures 1B and S1B), while *Krt19* protein expression localized to differentiated cells of the intestinal villus (Figure S1D). We have previously reported a progenitor/stem cell marker in the stomach that similarly displayed a discrepancy in the pattern between RNA versus protein expression

(Quante et al., 2010), so we sought to examine whether *Krt19* also marked a stem cell population. We developed a Krt19-BAC-mApple (*Krt19*-mApple) reporter mouse (Figure S1I), confirming that Krt19 gene expression was limited only to cells located well above the crypt base in both the colon (Figure 1C) and intestine (Figure 1D). Notably, the absence of both *Krt19* mRNA and protein expression from the crypt base (Figures 1A–1D; Figures S1A–S1H) afforded us the unique opportunity to selectively label and compare a progenitor/stem cell pool situated above the crypt base (position +4) to the well described *Lgr5*^{+} CBC cells (Barker et al., 2007) and the more recently reported *Lrig1*^{+} stem cells (Powell et al., 2012) found at the crypt base.

To identify an *Lgr5*-negative progenitor/stem cell pool in the colon, we established a genetic fate-mapping system for labeling *Krt19*. We generated a *Krt19*-BAC-*CreERT2* (*Krt19*-CreERT) transgenic line (Figures S1J and S1K) that was crossed to R26-LacZ (R26-LacZ) and ROSA26-mT/mG (R26-mT/mG) reporters in order to perform genetic lineage tracing experiments in homeostasis, inflammation, and cancer. Shortly following tamoxifen induction, β-galactosidase[+] (β-gal) cells were localized to the colonic crypt (Figure 1E) in a pattern identical to *Krt19*-expressing cells detected by in situ and *Krt19*-mApple^{+} cells detected using a *Krt19*-mApple transgenic reporter mouse. Twenty-four hours after tamoxifen, recombination was evident in the colonic isthmus, extending down to the +4 position, but distinctly above the crypt base (Figures 1G and S2A). One week following tamoxifen, recombined cells derived from *Krt19*^{+} cells extended downward to include *Lgr5*^{+} cells at the colonic crypt base (Figures 1G and S2A). Sixteen weeks post-induction, *Krt19*^{+} cells traced all epithelial cell lineages in the colon (Figures 1G and S2A), and completely labeled glands were detected without any loss of labeling beyond 52 weeks (Figure 1G; Figures S2A–S2D), consistent with *Krt19* labeling long-lived stem cells.

In vitro, two-photon florescence microscopy of colonic crypts isolated from *Krt19*- CreERT;R26-mT/mG mice 12 hr after a single dose of tamoxifen also revealed recombination (GFP+) in a number of *Krt19*-expressing cells above the crypt base (Figures 1I and 1J; n = 6, colon). These cells contained bona fide stem cells and gradually replaced all epithelial cells over 9–10 days (colon: Figures 1I and 1J).

Similarly, in the intestine, genetic lineage tracing experiments revealed that shortly following tamoxifen induction, Krt19-labeled β-gal^{+} cells located clearly above the crypt base in the intestinal crypt (Figures 1K and S2E). These cells eventually traced all intestinal epithelial cell lineages, including *Lgr5*^{+} cells at the crypt base (Figure 1K; Figures S2E and S2F), and again, consistent with the labeling of long lived stem cells, we observed no loss of labeling beyond 52 weeks (Figures 1C and 1D). Furthermore, in intestinal enteroids grown in vitro, a few *Krt19*^{+} cells above the crypt base could be detected 12 hr following tamoxifen (Figures S2G–S2I; n = 4, intestine), and these cells expanded over 9–10 days to replace the entire crypt-villus column (Figures S2G–S2I). Single-cell culture of *Krt19*-mApple^{+} cells isolated from the intestine of *Krt19*-mApple reporter mice further confirmed the stem cell capacity of *Krt19*^{+} cells (Figure S2J) at ∼1% clonogenic efficiency compared to 5% for Lgr5-GFP^{+} cells.

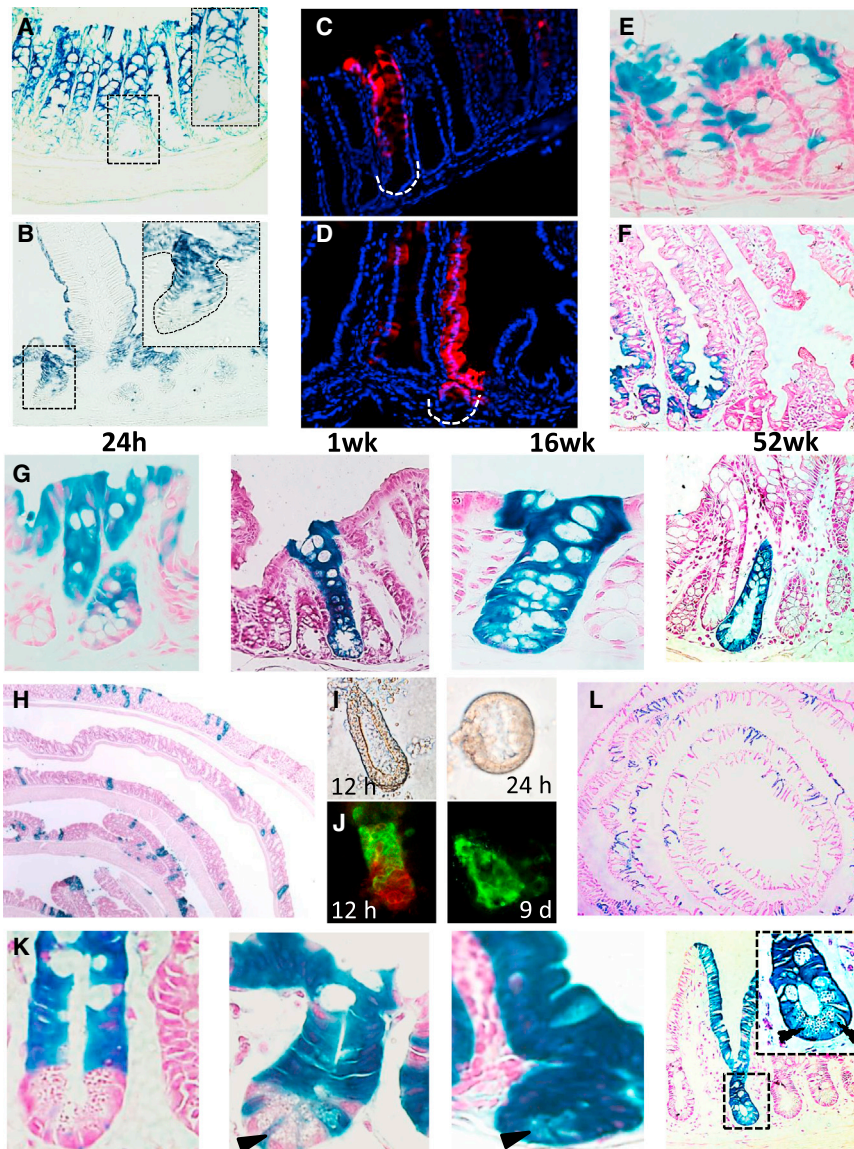**24h**   **1wk**   **16wk**   **52wk**

Figure 1. Krt19 mRNA Localizes to the Colonic and Intestinal Stem Cell Zone and Marks Long-Lived Stem Cells

(A and B) *Krt19* mRNA is expressed in the isthmus extending down to the +4 position of the colonic (A) and (B) intestinal crypt. High-magnification images of the crypt base are shown as insets.

(C and D) *Krt19*-mApple$^+$ cells in the colon (C) and small intestine (D) of *Krt19-mApple* reporter mice show expression similar to in situ.

(E and F) 24 hr post-tamoxifen, β-gal$^+$ colonic (E) and intestinal (F) crypts in *Krt19*-CreERT;R26R-LacZ mice also show expression identical to in situ.

(G) Lineage tracing in the colon of *Krt19*-CreERT;R26RLacZ mice. High-magnification images of the crypt base are shown at 24 hr and 52 weeks following tamoxifen (6 mg per os [p.o.]).

(H) Low-magnification images of lineage tracing in the colon of *Krt19*-CreERT;R26RLacZ 26 weeks following tamoxifen (n ≥ 7 per group).

(I and J) Bright-field (6 and 24 hr after culture) (I) and two-photon images (24 hr and 9 days following tamoxifen [6 mg p.o.]) (J) of colonic crypts from *Krt19*-CreERT; R26-mT/mG mice (n ≥ 4 per group) cultured in vitro.

(K) Lineage tracing in the intestine in *Krt19*-CreERT/R26RLacZ mice with high-magnification images of the crypt base shown at 24 hr to 52 weeks following tamoxifen (6 mg p.o.). Black arrows show Krt19-derived CBCs at 7 days and Paneth cells at 16 and 52 weeks.

(L) Low-magnification images of lineage tracing in the intestine of *Krt19*-CreERT/R26RLacZ 26 weeks following tamoxifen (n ≥ 7 per group).

See also Figures S1 and S2.

Krt19$^+$-Potential Stem Cells above the Crypt Base Are Distinct from *Lgr5*$^+$ CBCs

To measure the overlap of *Krt19*$^+$ cells with *Lgr5*$^+$ cells, we performed *Krt19* in situ hybridization on colonic (Figure 2A) tissues of *Lgr5*-EGFP-IRES-CreERT2 mice. We confirmed that *Krt19* mRNA expression was not detectable in CBC stem cells marked by *Lgr5* and overlapped rarely with a very small subset of *Lgr5*-GFP-positive cells located much higher in the colonic crypt (average position +7) (Figure 2C). Similarly, *Krt19* mRNA expression not detectable in *Lgr5*$^+$ CBCs in the intestine (Figure 2B) and again overlapped rarely with a very small subset of *Lgr5*-GFP-positive cells located much higher in the crypt (average position +7) (Figure 2C). The majority of *Krt19*$^+$ cells were also distinct from *Lgr5*$^+$ cells with respect to their proliferation status, as most *Lgr5*$^+$ cells were located immediately below the proliferation zone, whereas *Krt19*$^+$ cells predominated within the proliferation zone (~12% *Lgr5*$^+$/Ki67$^+$ versus ~50% *Krt19*$^+$/Ki67$^+$

cells) (Figures 2D–2F; Figures S3A–S3J). Importantly, when we generated *Krt19*-mApple;*Lgr5*-EGFP-IRES-CreERT2 dual reporter mice, *Krt19*-mApple$^+$/*Lgr5*-GFP$^+$ double-positive cells were only detected in extremely rare cells located higher in the colonic crypt (Figure 2G) and comprised <0.05% of total epithelial cells and <6% of Lgr5-GFP$^+$ cells as detected by FACS (Figures 2I and 2J; Figure S3K). Similarly, in the intestine, <0.01% of total epithelial cells and <5% of Lgr5-GFP$^+$ cells were *Krt19*-mApple$^+$/*Lgr5*-GFP$^+$ double-positive cells as determined by imaging (Figure 2H) and fluorescence-activated cell sorting (FACS) analysis (Figures 2J and S3K). Thus, *Krt19* and *Lgr5* identify largely distinct populations (Figure 2K), with only rare overlap near the +7 cell region.

Interestingly, RNA expression analysis revealed that the *Krt19*-mApple$^+$/ *Lgr5*-GFP$^+$ double-positive intestinal cells displayed significant enrichment for the known "+4" intestinal stem cell markers *Bmi1*, *Hopx*, and *Lrig1*, as well as the intestinal progenitor marker *Dll1* (Figure 2L), whereas *Lgr5*-negative *Krt19*-mApple$^+$ cells showed relatively low or undetectable levels of both "+4" stem cell and progenitor markers (Figure 2L). Remarkably, despite the heterogeneity of *Krt19*$^+$ cells posing a potential confounding factor in this RNA expression analysis, we
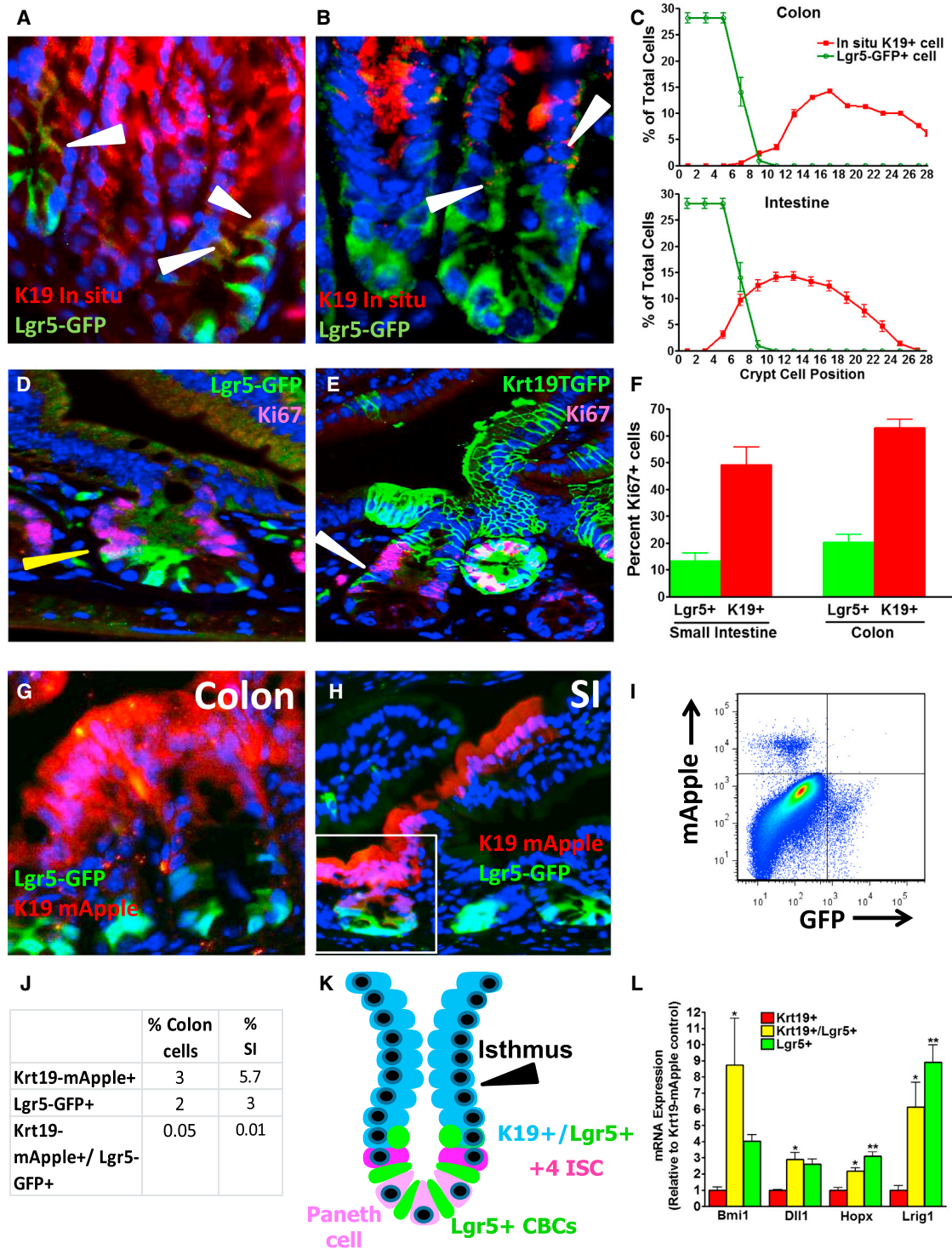
A

K19 In situ
Lgr5-GFP

B

K19 In situ
Lgr5-GFP

C Colon

In situ K19+ cell
Lgr5-GFP+ cell

% of Total Cells

Intestine

% of Total Cells

Crypt Cell Position

D

Lgr5-GFP
Ki67

E

Krt19TGFP
Ki67

F

Percent Ki67+ cells

| Lgr5+ | K19+ | Lgr5+ | K19+ |
Small Intestine   Colon

G Colon

Lgr5-GFP
K19 mApple

H SI

K19 mApple
Lgr5-GFP

I

mApple

GFP

J

	% Colon cells	% SI
Krt19-mApple+	3	5.7
Lgr5-GFP+	2	3
Krt19-mApple+/ Lgr5-GFP+	0.05	0.01

K

Isthmus

K19+/Lgr5+
+4 ISC

Paneth cell

Lgr5+ CBCs

L

mRNA Expression
(Relative to Krt19-mApple control)

Krt19+
Krt19+/Lgr5+
Lgr5+

Bmi1   Dll1   Hopx   Lrig1

Figure 2. Krt19+ Cells Are Located above Lgr5+ Crypt Base Columnar Cells in the Colon and Intestine

(A and B) Colocalization of *Krt19* mRNA-expressing cells (red) detected by in situ, and Lgr5-GFP+ cells (green) in the colon (A) and small intestine (B) of *Lgr5*-EGFP-IRES-CreERT2 mice. White arrows denote double-positive cells.

(C) Average cell position of *Krt19* mRNA-expressing (red) and *Lgr5*-EGFP+ (green) cells within the colonic (top panel) and intestinal (bottom panel) crypt.

(D and E) Colocalization of Ki67 and *Lgr5*-EGFP+ cells (D) versus Ki67 and *Krt19*-EGFP+ cells 12 hr after tamoxifen (E) in *Lgr5*-EGFP-IRES-CreERT2 or *Krt19*-CreERT;ROSA26-mG/mT mice, respectively. Yellow arrow shows a rare double-positive (Ki67+, Lgr5-GFP+) cells, and white arrow shows a rare Krt19+, Ki67− cells.

(F) Quantification of double-positive Ki67+Krt19+ cells (red bars) versus Ki67+Lgr5-GFP+ cells (green bars).

(legend continued on next page)

confirmed using microscopy that only rare *Krt19*^{+}/*Bmi1*^{+} cells are detected in the crypts of *Krt19*-CreERT;ROSA26-Tomato mice crossed to *Bmi1*-GFP mice (Figure S3L).

Thus, given the infrequent overlap of *Krt19* and *Lgr5*, we sought to definitively distinguish between *Krt19*^{+} versus Lgr5^{+} cells. We generated *Lgr5*-DTR-EGFP;*Krt19*-CreERT;R26-Tomato mice to conditionally ablate *Lgr5*^{+} cells following administration of diphtheria toxin, as previously described (Tian et al., 2011). First, we confirmed at 24 hr following tamoxifen induction that *Krt19*-Tomato^{+} cells were located above the crypt base and were almost entirely distinct from *Lgr5*-GFP[+] CBCs (Figures 3A and 3B). Next, we administered diphtheria toxin (DT) 3 days prior to tamoxifen in order to ablate *Lgr5*^{+} cells before the start of *Krt19* lineage tracing (Figure 3C). Interestingly, *Krt19*^{+} colonic stem cells continued to lineage trace in the colon and gave rise to new *Lgr5*-GFP^{+} cells when the diphtheria toxin was stopped (Figure 3D). Importantly, the efficiency of *Krt19*^{+} cell-lineage tracing was unchanged despite *Lgr5*^{+} cell ablation effectively eliminating both the *Lgr5*-GFP[+] CBCs, as well as the rare "+4" *Krt19*-mApple[+]/*Lgr5*-GFP[+] double-positive cell populations (Figure 3E).

Similarly, *Krt19*^{+} cells in the intestine continued to lineage trace and display resiliency in the face of *Lgr5*-GFP[+] cell ablation (Figure 3D). From these data, we conclude that *Krt19*^{+} lineage tracing in the intestine was not due to overlap with the *Dll1*^{+} progenitor population for several reasons. First, *Dll1* RNA expression was predominantly detected within the rare "+4" *Krt19*-mApple[+]/*Lgr5*-GFP[+] double-positive and *Lgr5*-GFP[+] CBC populations, rather than within *Krt19*-mApple^{+} cells. Moreover, *Dll1*^{+} progenitors are reported to show no lineage tracing capacity when irradiated 2 weeks after tamoxifen (van Es et al., 2012) and, additionally, are unable to form intestinal enteroids in the absence of Wnt3a (van Es et al., 2012). In contrast, *Krt19*^{+} cells formed intestinal enteroids in the absence of Wnt3a (Figures S4A–S4C) and also showed lineage tracing capacity in vivo when irradiated 2 weeks after tamoxifen (Figures 4K and 4L).

Krt19[+] lineage tracing capacity was not due to overlap with *Krt19*^{+} transit-amplifying (TA) cells. We used 5-fluorouracil (5-FU) to target the rapidly proliferating TA cell population as previously described (Doetsch et al., 1999; Stange et al., 2013) and confirmed that this treatment eliminated nearly all (> 95%) of the proliferating TA cells in both the colon and intestine (Figures 3F–3H; Figure S4D). *Krt19*^{+} cells lineage traced with the same efficiency in both the colon and intestine regardless of TA cell ablation alone, or TA cell plus *Lgr5*^{+} cell ablation (Figures 3I and 3J). Taken together, these data prove that *Krt19* identifies a novel *Lgr5*(−) *Krt19*-expressing potential stem cell population in both the colon and intestine. Interestingly, *Krt19*

and *Lgr5* additionally label distinct cell populations during development. Using a newly generated, constitutive *Krt19*-BAC-CRE transgenic mouse, we observed that *Krt19* marked the early gastrointestinal endoderm, raising the possibility that *Krt19* may also label a stem cell population in development (Figures S5A–S5G). This is in contrast to *Lgr5*-GFP^{+} cells, which were first detected in the intestine as weakly GFP+ cells on post-natal day 5 (Figures S5H and S5I).

Krt19[+] Cells Show Relative Radioresistance and Are Functionally Distinct from *Lgr5*^{+} Stem Cells and *Dll1*^{+} Progenitors

Radiation injury initiates intestinal stem cell division during epithelial repair (May et al., 2008; Yan et al., 2012), but *Lgr5*^{+} stem cells have been proposed to be radiosensitive (van Es et al., 2012; Yan et al., 2012), whereas *Bmi1*^{+} stem cells are radioresistant (Yan et al., 2012). Thus, we sought to compare *Krt19*^{+} versus *Lgr5*^{+} stem cells with respect to their sensitivity to radiation. *Krt19*-CreERT;R26-LacZ and *Lgr5*-EGFP-IRES-CreERT2;R26-LacZ mice were irradiated (12 Gy) 24 hr following tamoxifen labeling of each cell population (Figure 4A). When *Lgr5*-EGFP-IRES-CreERT2;R26-LacZ mice were irradiated 24 hr after tamoxifen, absence of lineage tracing (Figures 4B and 4D; Figure S6A) immediately following and in the early post-radiation period confirmed that *Lgr5*^{+} cells were radiosensitive (Yan et al., 2012). Consistent with *Lgr5*^{+} cell radiosensitivity, we observed a loss of *Lgr5*-GFP expression immediately following radiation (Figure 4E). In contrast, radioresistant *Krt19*^{+} cells continued to lineage trace in irradiated *Krt19*-CreERT;R26-LacZ mice (Figures 4C and S6B), and we detected an increase in contiguously labeled *Krt19*^{+} crypts, consistent with crypt fission (Figure 4D) and stem cell expansion through symmetric division as previously described (Park et al., 1995). Moreover, the conclusion that radioresistance of *Krt19*^{+} cells was due to the labeling of stem cells, rather than TA cells, was supported by our observations that targeting of TA cells with 5-FU prior to radiation did not alter the lineage tracing capacity of *Krt19*^{+} cells (Figures 4G and 4H). *Krt19*^{+} cells also showed longevity (>18 months) well beyond the 2 week life span of *Dll1*^{+} progenitors and, importantly, showed lineage tracing capacity even when irradiated 2 weeks following tamoxifen induction (Figures S6E and S6F).

To confirm our in vivo observations, we examined the effects of radiation on intestinal enteroid growth and stem cell function in vitro (Figure 4I). Following 10 Gy irradiation, intestinal enteroids from *Krt19*-mApple[+]/*Lgr5*-GFP[+] dual reporter mice showed a marked reduction in *Lgr5*-GFP^{+} stem cells associated with the loss of crypt budding, suggesting crypt injury (Figures 4I and 4J). In contrast, the same enteroids showed that *Krt19*-mApple-expressing cells remained radioresistant and survived
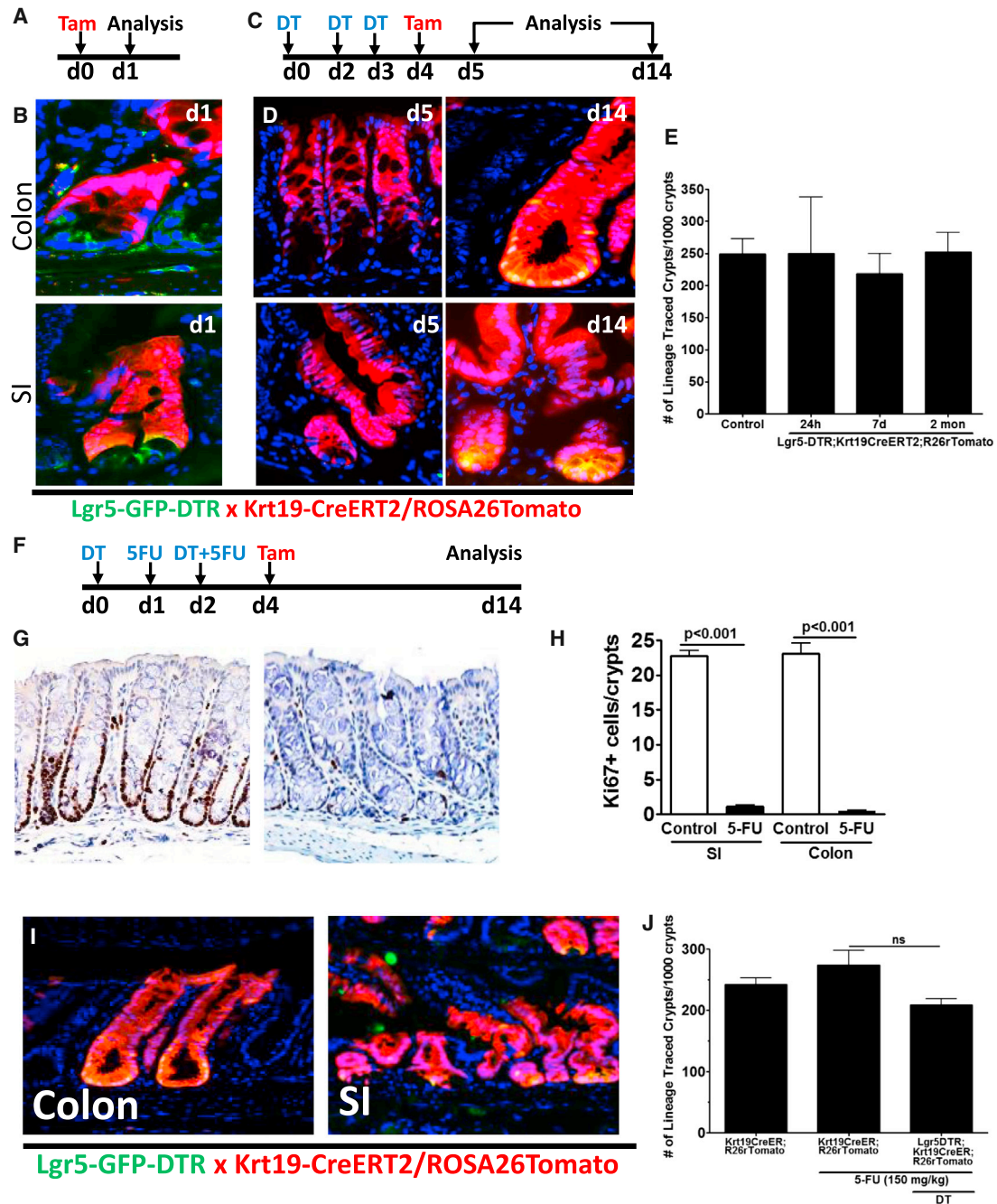
Figure 3. *Krt19*^{+} Stem Cells Render *Lgr5*^{+} Stem Cells Dispensable in the Colon and Small Intestine
(A) Tamoxifen protocol used to analyze *Krt19*^{+} and *Lgr5*^{+} cells in *Lgr5*-DTR-EGFP;*Krt19*-CreERT/R26RTomato mice 24 hr post-tamoxifen.
(B) Images of the colon and SI 24 hr post-tamoxifen are shown.
(C and D) Diphtheria toxin (DT) ablation regimen (C) used in *Lgr5*-DTR-EGFP;*Krt19*-CreERT/R26RTomato mice showing *Krt19*^{+} stem cells (red) render *Lgr5*^{+} cells (green) dispensable in the colon and SI (D).
(E) Quantification of *Krt19*^{+} stem cell lineage tracing efficiency in the presence or absence of *Lgr5*^{+} stem cells is shown.
(F) DT-induced *Lgr5*^{+} cells ablation and 5-FU-induced transit-amplifying (TA) cell ablation regimen used in *Lgr5*-DTR-EGFP;*Krt19*-CreERT/R26RTomato mice.
(G) Representative high-power view of Ki67^{+} cells in the colon of control (left) versus 5-FU-treated (right) mice.
(H) Quantification of Ki67^{+} cells in the colon or intestine of control versus 5-FU-treated mice.
(I) *Krt19*^{+} stem cells (red) render *Lgr5*^{+} cells (green) dispensable in the colon and SI in spite of 5-FU ablation of TA cells.
(J) Quantification of *Krt19*^{+} stem cell lineage tracing efficiency in the presence or absence of *DT* and/or 5-FU stem cells (I) is shown (n ≥ 6 per group).
Data in all bar graphs are presented as mean ± SEM.
See also Figures S4 and S5.

radiation injury. Indeed, during the regenerative state post-radiation, newly budding crypts arose from radioresistant $Krt19$-mApple-labeled cells (Figure 4J). These data again confirmed our in vivo observations that $Krt19^+$ cells show relative radioresistance when compared to $Lgr5^+$ stem cells.

Recently, it was shown that interconversion can occur between $Hopx^+$ and $Lgr5^+$ cells in vitro (Takeda et al., 2011) and that $Dll1^+$ progenitors can also revert back to an $Lgr5^+$ state in vitro (van Es et al., 2012). Thus, we examined whether radiosensitive $Lgr5^+$ stem cells could give rise to radioresistant stem cells in vivo. When we allowed for $Lgr5$ lineage tracing to occur for up to 2 weeks prior to radiation (12 Gy) exposure, we observed a significant increase in the number of contiguously labeled $Lgr5$ traced SI crypts in $Lgr5$-EGFP-IRES-CreERT2;R26-LacZ mice after radiation (Figures 4K–4N; Figures S6C and S6D). Lineage tracing from $Lgr5^+$ cells was only observed when tamoxifen was administered at least 2 weeks prior to radiation, suggesting that $Lgr5^+$ cells can over time give rise to a radioresistant stem cell population, such as $Krt19^+$ cells. We demonstrated that $Krt19^+$ cells give rise to $Lgr5^+$ cells (Figures 1G and 1K; Figures S2A and S2E); thus, to our knowledge, this is the first in vivo evidence that stem cell interconversion readily occurs between radioresistant ($Krt19^+$) and radiosensitive ($Lgr5^+$) states.

Radioresistant $Krt19^+$ Cancer-Initiating Cells Are Functionally Distinct from $Lgr5^+$ Cells

The contribution of $Lgr5^+$ stem cells to early tumor development has previously been demonstrated by the formation of intestinal adenomas upon targeted mutation of the Apc gene in this lineage (5). However, the contribution of additional stem cell pools to the origin of cancer remains unknown. To determine whether $Krt19^+$ cells can also function as cancer-initiating cells in the colon and intestine, we generated $Krt19$-CreERT;R26-LacZ;Apc$^{F/F}$ mice in which conditional expression of a truncated form of Apc occurs in $Krt19^+$ cells following tamoxifen induction. Analogous to $Lgr5^+$ stem cells, $Krt19^+$ cells initiated intestinal tumorigenesis following Apc deletion, resulting in rapid mortality (Figure 5A). To functionally distinguish between $Krt19^+$ and $Lgr5^+$ cancer-initiating cells, however, we further compared the susceptibility of these two stem cell pools to radiation injury. Interestingly, when irradiated 24 hr after tamoxifen, $Lgr5$-EGFP-IRES-CreERT2;R26-LacZ;Apc$^{F/F}$ mice showed no mortality (Figure 5B) and normal non-lineage-traced colon and intestine (Figure 5C), whereas similarly treated $Krt19$-CreERT;R26-LacZ;Apc$^{F/F}$ mice continued to display rapid mortality (Figure 5B) from numerous lineage traced colonic and intestinal tumors (Figure 5D). Taken together, these observations provide evidence that $Krt19^+$ stem cells are cancer-initiating cells distinct from $Lgr5^+$ cells.

Furthermore, when crypts from $Krt19$-CreERT; R26-mT/mG;Apc$^{F/F}$ mice were cultured in vitro 24 hr after tamoxifen, recombined Apc floxed $Krt19^+$ cells appeared as GFP$^+$ spheroid structures (Figures 5E and 5F), which were easily distinguishable from non-recombined crypts that remained Tomato$^+$ and formed normal budding crypt structures. Consistent with our in vivo observations, following in vitro irradiation (10 Gy), Apc floxed $Krt19^+$ spheroids were radioresistant with no change in growth, and non-recombined Apc wild-type crypts showed radiosensitivity only within the budding crypts that contain $Lgr5^+$ stem cells

(Figures 5G–5I). Post-radiation, there was neither in vitro nor in vivo $Lgr5$ mRNA expression, while $Krt19$ mRNA actually increased (Figures 5J and 6A). Thus, radiosensitive $Lgr5^+$ stem cells are dispensable in both normal and Apc mutated crypts. Similarly, in Apc floxed tumors of $Lgr5$-EGFP-IRES-CreERT2;R26-LacZ;Apc$^{F/F}$ mice, we detected reduced $Lgr5$-GFP$^+$ cells, but unchanged $Krt19$ protein-positive cells 24 hr post-radiation (Figures 6B and 6C).

When we additionally performed DT ablation of $Lgr5^+$ cancer stem cells in crypts from $Lgr5$-DTR-EGFP;$Krt19$-CreERT;R26-LacZ;Apc$^{F/F}$ mice, we observed continued growth of many, but not all, $Krt19^+$ Apc floxed enteroids (Figures 6D–6F). We confirmed the efficacy of DT ablation of $Lgr5^+$ cells by the absence of $Lgr5$ mRNA expression (Figure 6G), which again was associated with a corresponding increase in $Krt19$ mRNA expression (Figure 6G). Importantly, $Krt19^+$ Apc floxed enteroids could also be maintained in culture in the absence of R-spondin and were completely unaffected even by $Lgr5^+$ cell ablation in this setting (Figures 6H and 6I). These data prove, for the first time, that $Krt19^+$ cell-derived Apc floxed enteroids are heterogeneous, with $Lgr5^+$ cancer stem cells being completely dispensable in these enteroids (Figures 6I and 6J).

DISCUSSION

In contrast to the intestine, the paucity of stem cell markers in the colon has hampered our ability to identify and adequately characterize $Lgr5$-negative stem cell pools in normal and neoplastic colonic crypts. Here, we show that $Krt19$-expressing cells, extending from the +4 position to the crypt isthmus, include unique long-lived stem cells that are distinct from $Lgr5^+$ CBCs. The distinct nature of $Krt19^+$ versus $Lgr5^+$ stem cells was confirmed by the observation that $Krt19^+$ cells continue to lineage trace crypts despite ablation of $Lgr5^+$ stem cells in both the colon and intestine. $Krt19^+$ cells actively contribute to normal epithelial maintenance and are also clearly functionally distinct from $Lgr5^+$ stem cells by their relative radioresistance. The radioresistance of $Krt19^+$ cells holds true not only in the colon but also in the intestine. Recognizing that $Krt19$-expressing cells comprise a heterogeneous population that also includes progenitor and TA cells, we confirmed that the differences in radiation response were nonetheless attributable to $Krt19^+$ stem cells. Indeed, the combination of TA cell targeting by 5-FU and DT ablation of $Lgr5^+$ cells confirmed that a unique population of $Krt19^+$ stem cells continue to lineage trace and expand following radiation injury. Notably, in the intestine, it has been shown that $Dll1^+$ progenitors and $Bmi1^+$ stem cells are radioresistant (van Es et al., 2012; Yan et al., 2012), while $Lgr5^+$ stem cells are radiosensitive. Interestingly, our observations regarding $Krt19^+$ cell radioresistance now extend these findings to the colon, where $Bmi1^+$ and $Dll1^+$ cells are not found (Sangiorgi and Capecchi, 2008; van Es et al., 2012). Moreover, $Krt19^+$ cells lineage trace independent of $Lgr5^+$ cells following radiation injury, as $Lgr5^+$ stem cells are radiosensitive when irradiated 24 hr following tamoxifen induction. Taken together with the recent observations of Metcalfe et al. (2014), the rapid regeneration of $Lgr5^+$ cells in the immediate post-radiation period is essential for epithelial repair and likely to occur from a radioresistant $Krt19^+$ population. Thus, long-lived radioresistant
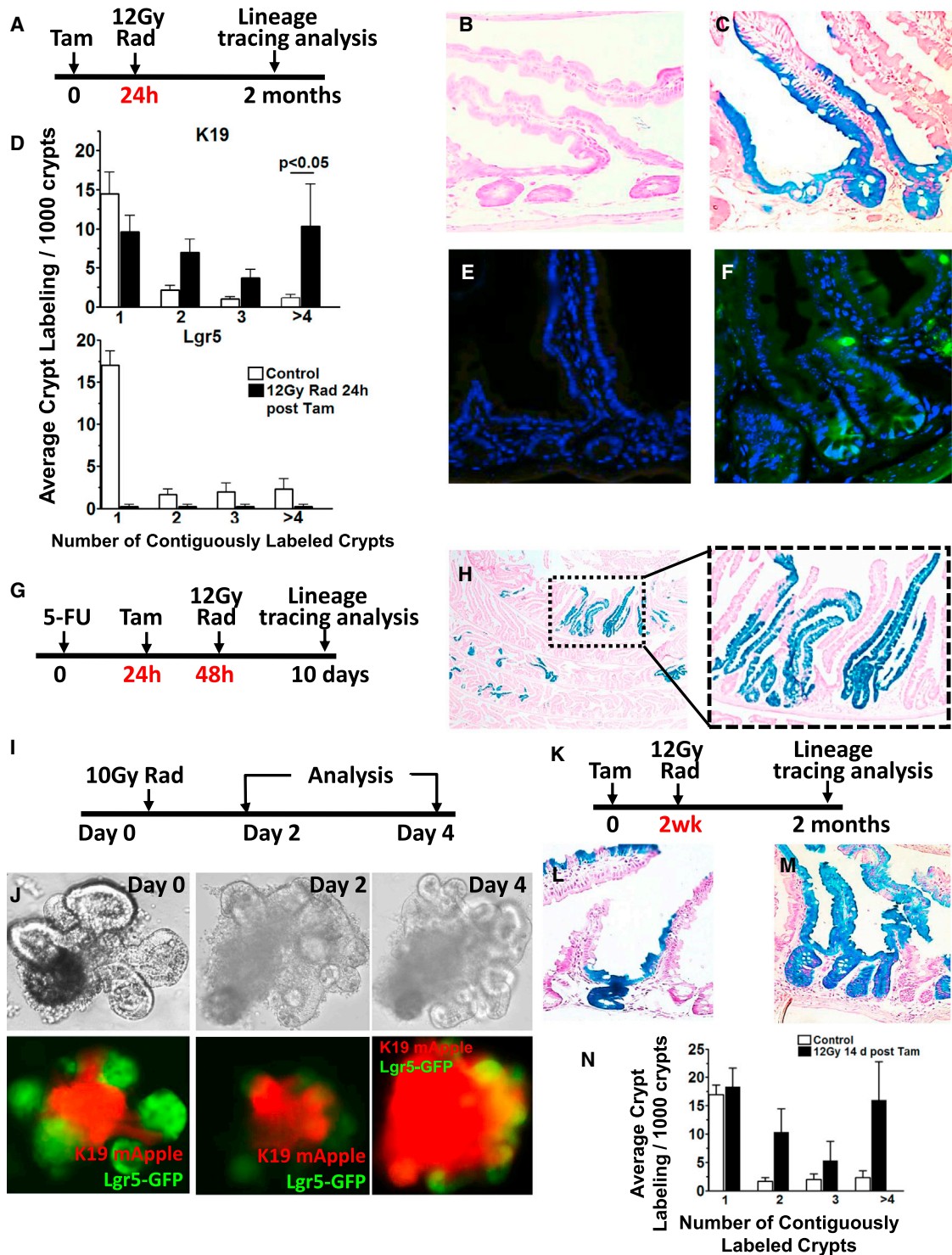
Figure 4. *Krt19*^{+} Cells Expand in Response to Injury and Display Relative Radioresistance Compared to *Lgr5*^{+} Stem Cells

(A) To examine the radiosensitivity of *Krt19*^{+} and *Lgr5*^{+} stem cells, mice were irradiated 24 hr after tamoxifen, and lineage tracing was examined 2 months following tamoxifen.

(B and C) Representative β-gal[+] intestinal crypts in *Lgr5*-EGFP-IRES-CreERT2;R26RLacZ (B) versus *Krt19-CreERT*;R26RLacZ (C) mice irradiated (12 Gy) 24 hr post-tamoxifen.

(D) Quantification of contiguously labeled β-gal[+] *Krt19* (top) versus *Lgr5*- (bottom) labeled crypts following irradiation 24 hr after tamoxifen.

(E and F) Representative small intestinal crypt-villus image of *Lgr5*-EGFP-IRES-CreERT2;R26RLacZ mice following high-dose radiation exposure demonstrating the disappearance of Lgr5-EGFP[+] crypt-based columnar cells 24 hr following irradiation (E) and re-emergence of EGFP[+] CBCs 7 days following irradiation (F).

(legend continued on next page)
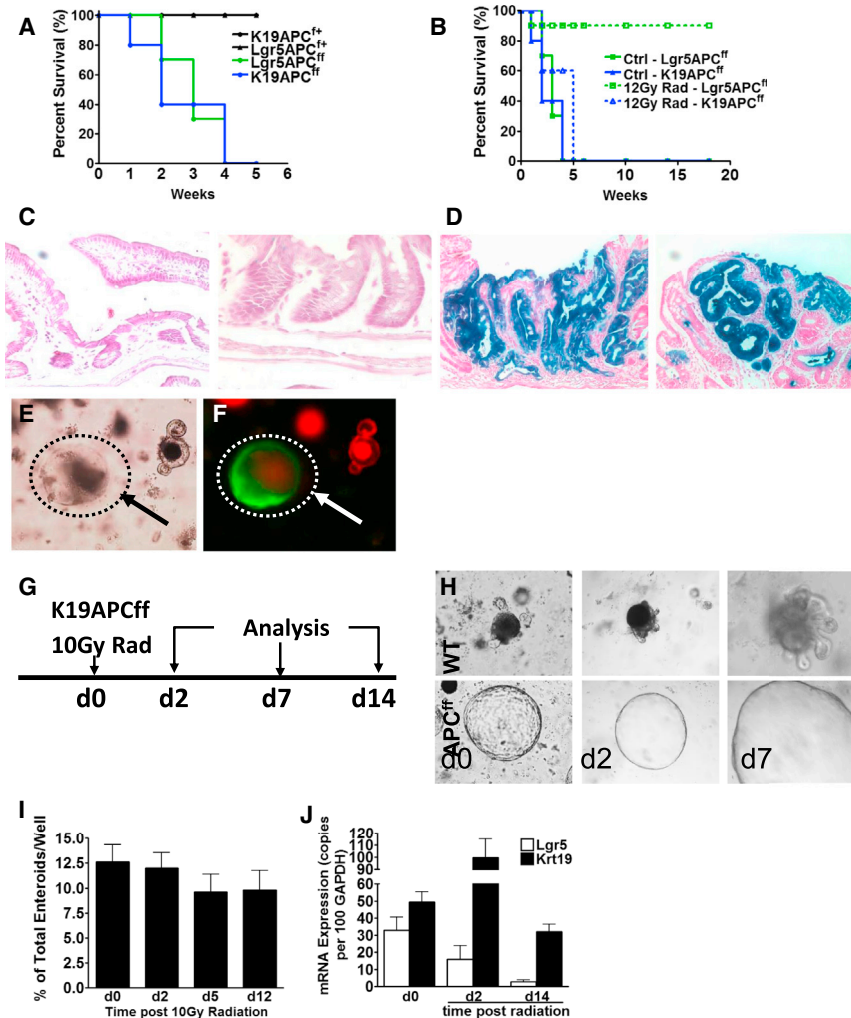
Figure 5. Radioresistant *Krt19*^{+} Cancer-Initiating Cells Are Functionally Distinct from *Lgr5*^{+} Stem Cells

(A) *Krt19*^{+} and *Lgr5*^{+} stem cells both serve as cancer-initiating cells, resulting in rapid mortality in *Krt19*-CreERT;R26-LacZ;ApcF/F or *Lgr5*-EGFP-IRES-CreERT2;R26-LacZ;ApcF/F mice.

(B–D) *Lgr5*-EGFP-IRES-CreERT2;R26-LacZ;ApcF/F mice irradiated 24 hr after tamoxifen show no mortality (B) and normal non-lineage-traced intestine (left) and colon (right) (C). In contrast, *Krt19*-CreERT;R26-LacZ;ApcF/F mice irradiated 24 hr after tamoxifen continue to show rapid mortality (B) from intestinal (left) and colonic (right) tumors (D); (n ≥ 6 per group).

(E and F) Bright-field (E) and fluorescent (F) images of intestinal crypts from *Krt19*-CreERT;R26-mT/mG;ApcF/F cultured in vitro 24 hr after tamoxifen. Arrows point to recombined GFP[+] *Apc* floxed *Krt19*^{+} cells appearing as spheroid structures.

(G) In vitro radiation protocol used to examine the effects of radiation injury on intestinal *Krt19*^{+} cell-derived *Apc* floxed tumor populations.

(H) *Krt19*^{+} cell-derived *Apc* floxed tumor populations pre- (day 0) and post- (day 2 and day 7) radiation (10 Gy).

(I) Quantification of surviving *Krt19*^{+} cell-derived APC floxed enteroids pre- and post-radiation injury.

(J) *Krt19* and *Lgr5* mRNA expression levels in *Krt19*^{+} cell-derived *Apc* floxed enteroids pre- and post-radiation injury.

Data in all bar graphs are presented as mean ± SEM.

Krt19^{+} cells are functionally distinct from radiosensitive *Lgr5*^{+} CBCs in both the colon and intestine.

Recent work by Takeda et al. (2011) suggested that interconversion between two or more stem cell pools occurs in enteroid cultures. Here, we demonstrate that *Krt19*^{+} stem cells give rise to *Lgr5*^{+} CBCs in both the colon and intestine and that the reverse is also true. That is, radiosensitive *Lgr5*^{+} stem cells give rise to *Krt19*^{+} radioresistant cells, given enough time to interconvert following tamoxifen. Therefore, although previously speculated to be true, we provide the first in vivo evidence that *Lgr5*^{+} cells

can indeed give rise to a radioresistant stem cell population (Figures 4 and S6).

Although the colon was the predominant focus of the current study, the potential overlap of *Krt19* with other +4 intestinal stem cell markers or *Dll1*^{+} progenitors raises the possibility that some of our observations in the intestine could be attributed to overlap with these cell populations. It is important to note, however, that intestinal *Krt19*^{+} cells are long lived, survive well beyond 18 months, and show lineage tracing capacity even when irradiated 2 weeks following tamoxifen induction. This is true, not only in the colon but also in the intestine, where this is in sharp contrast to intestinal *Dll1*^{+} progenitors that are short lived and do not display any lineage tracing capacity

(G) In vivo 5-FU (150 mg/kg) protocol used to examine the effects of TA cell ablation on *Krt19*^{+} stem cell lineage tracing.

(H) Representative low (left) and high (right) power images of *Krt19*^{+} cell lineage tracing in *Krt19*-CreERT;R26RLacZ mice treated with 5-FU and examined 8 days post-radiation.

(I) In vitro radiation protocol used to examine the effects of radiation injury on intestinal *Krt19* and *Lgr5* stem cell populations.

(J) Bright-field (top) and fluorescent (bottom) images of intestinal enteroids from *Krt19*-mApple[+]/ *Lgr5*-GFP[+] double transgenic mice cultured in vitro pre- and post-radiation (10 Gy).

(K) Radiation protocol used to examine *Lgr5*-derived lineage tracing in *Lgr5*-EGFP-IRES-CreERT2/R26RLacZ mice 2 weeks after tamoxifen.

(L and M) β-gal[+] intestinal crypts from control (L) versus irradiated (M) *Lgr5*-EGFP-IRES-CreERT2;R26RLacZ mice.

(N) Quantification of contiguously labeled β-gal[+] *Lgr5*-labeled crypts following irradiation 2 weeks after tamoxifen; (n ≥ 5 per group).

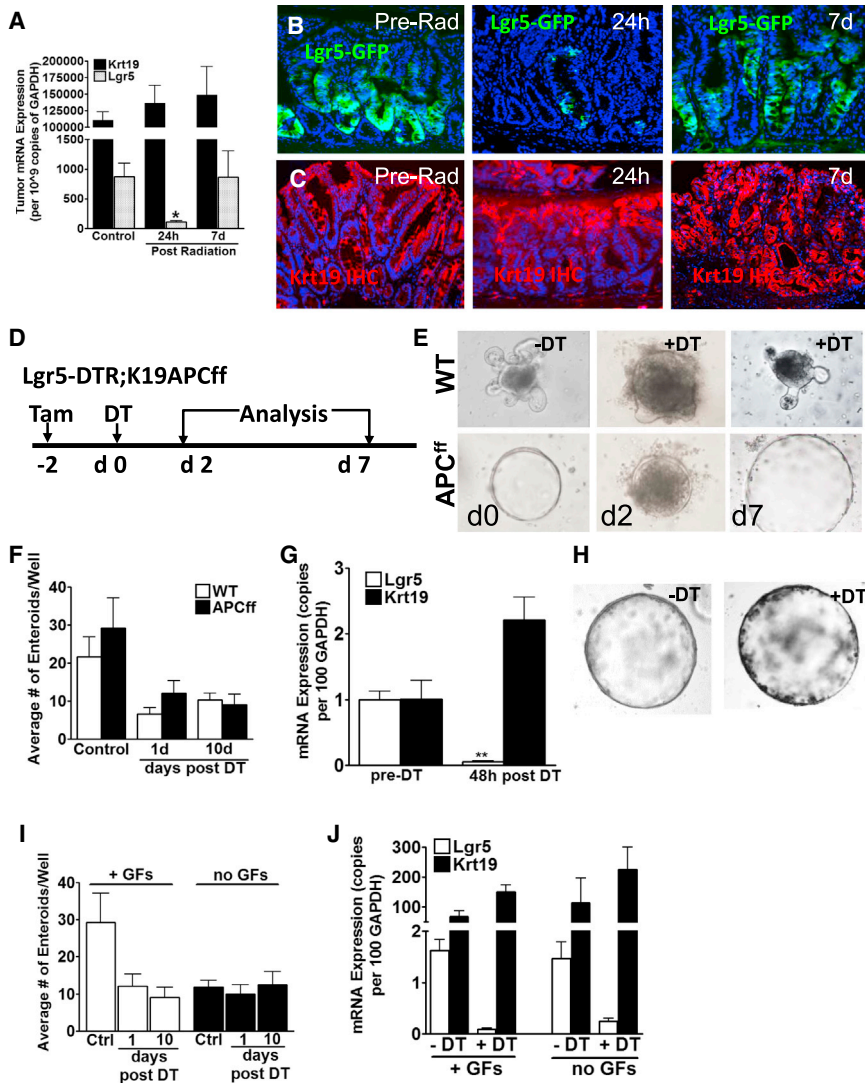Data in all bar graphs are presented as mean ± SEM.

See also Figure S6.

Figure 6. Lgr5^{+} Stem Cells Are Radiosensitive within Colonic Tumors, Unlike Krt19^{+} Cells, which Are Radioresistant

(A) In vivo *Krt19* and *Lgr5* mRNA in *Apc* floxed tumors pre- or post- (24 hr and 7 days) radiation; * indicates p < 0.05 versus control; (n ≥ 4 per group).

(B and C) *Lgr5*-GFP[+] (B) and *Krt19* immunopositive (C) cells in *Apc* floxed tumors pre- or post-radiation-induced targeting of *Lgr5*^{+} cells.

(D) In vitro *Lgr5*^{+} cell ablation protocol used to examine the dispensability of *Lgr5*^{+} cells in *Krt19*^{+} cell-derived *Apc* floxed enteroids from *Lgr5*-EGFP-DTR;*Krt19*-CreERT;Apc[F/F] mice.

(E) Bright-field images of intestinal enteroids from *Lgr5*-EGFP-DTR;*Krt19*-CreERT;Apc[F/F] mice pre- (day 0) and post- (day 2 and day 7) DT ablation of *Lgr5*^{+} cells.

(F) Quantification of surviving *Krt19*^{+} cell-derived WT and APC floxed enteroids pre- and post-*Lgr5*^{+} cell ablation.

(G) *Krt19* and *Lgr5* mRNA expression levels in *Krt19*^{+} cell-derived APC floxed enteroids pre- and post- (48 hr) *Lgr5*^{+} cell ablation (G); ** indicates p < 0.01 versus control; (n ≥ 4 per group).

(H) Bright-field images of *Krt19*^{+} cell-derived APC floxed intestinal enteroids from *Lgr5*-EGFP-DTR;*Krt19*-CreERT;Apc[F/F] mice cultured in the presence (−DT) or absence (+DT) of *Lgr5*^{+} cell ablation.

(I) Quantification of surviving *Krt19*^{+} cell-derived APC floxed enteroids pre- and post-*Lgr5*^{+} cell ablation and cultured in the presence/absence of growth factors.

(J) *Krt19* and *Lgr5* mRNA expression levels in *Krt19*^{+} cell-derived APC floxed enteroids grown in the presence or absence of standard growth factors (R-spondin and noggin), pre- and post- (48 hr) *Lgr5*^{+} cell ablation; (n ≥ 4 per group).

Data in all bar graphs are presented as mean ± SEM.

when irradiated beyond 24 hr following tamoxifen (van Es et al., 2012). Moreover, *Krt19*^{+} cells remained capable of sustaining intestinal enteroids in vitro, despite ablation of *Lgr5*^{+} stem cells and the absence of Wnt3a (a factor recently shown to be essential for *Dll1*^{+} progenitor reversion to stem cells). Furthermore, our RNA expression analysis revealed that the overlap of *Krt19* with the various +4 intestinal stem cell markers, as well as *Dll1*, was only true of rare *Krt19*^{+}/*Lgr5*^{+} double-positive cells above the CBCs, yet DT ablation of all *Lgr5*^{+} cells, including this overlapping population had no effect on *Krt19*^{+} stem cell lineage tracing activity. Taken together, these data prove that overlap with *Dll1*^{+} progenitors and *Bmi1*^{+} stem cells cannot solely explain our observations regarding radioresistance of *Krt19*^{+} cells in the intestine.

Ritsma et al. (2014) recently suggested that *Lgr5*^{+} cells display heterogeneity based on their "border" versus "central" position within the intestinal crypt. Our own observations that a rare subset of *Lgr5*^{+} cells expresses *Krt19*, while the majority of *Lgr5*^{+} cells do not, supports the premise of heterogeneity among *Lgr5*^{+} cells and, additionally, leads one to speculate whether

Krt19-mApple[+]/ *Lgr5*-GFP[+] double-positive cells identify a unique subset of *Lgr5*^{+} cells with "potential" stem cell activity as previously described (Kozar et al., 2013).

Conditional expression of a truncated form of *Apc* additionally confirmed that *Krt19*^{+} cells include a population of cancer-initiating cells. That cancer initiation in *Lgr5*-EGFP-IRES-CreERT2;R26-LacZ;Apc[F/F] mice was completely suppressed in the colon, as well as the intestine, by high-dose radiation 24 hr following tamoxifen confirmed that *Lgr5*^{+} cancer-initiating cells were radiosensitive. In contrast, similarly treated *Krt19*-CreERT;R26-LacZ;Apc[F/F] mice developed many colonic and intestinal tumors despite irradiation, again demonstrating the functional distinction of *Krt19*^{+} versus *Lgr5*^{+} cancer-initiating cells. Thus, we provide the first definitive evidence of an *Krt19*^{+}/*Lgr5*(−) radioresistant cancer-initiating cell population in both the colon and intestine. In view of the high prevalence of colon cancer and inflammatory conditions affecting the colon, the identification of colonic *Krt19*^{+}/*Lgr5*(−) cancer-initiating stem cells is highly relevant to our understanding and treatment of human disease. Additionally, we now demonstrate that *Lgr5*^{+}

cancer stem cells are dispensable in *Apc* floxed tumors, particularly in R-spondin-independent conditions. In view of the recent findings that R-spondin fusion proteins activate Wnt signaling in a subset of human colorectal tumors, our observations may have important implications for *Lgr5*^{+} cell-targeted therapy in subsets of colorectal cancer patients (Seshagiri et al., 2012).

In summary, we identify a novel population of colonic *Krt19*^{+} cells that give rise to *Lgr5*^{+} CBC cells. Radioresistant *Krt19*^{+} cells located above the crypt base can initiate cancer and are functionally distinct from radiosensitive *Lgr5*^{+} CBCs. These findings have important clinical relevance for future cancer therapy targeting colonic stem cell populations.

EXPERIMENTAL PROCEDURES

Generation of *Krt19*-CreERT2 Transgenic Mice
For BAC recombineering, the K19 containing BAC clone (BAC RP-23-24N13) was transformed into SW105 competent cells and a *Krt19*-BAC-CreERT2 construct generated by BAC recombineering. All animal studies were performed in Institutional Animal Care and Use Committee (IACUC)-approved facilities and completed in accordance to IACUC protocols at Columbia University. See Supplemental Experimental Procedures for further details.

Lineage Tracing Analysis, Assessment, and Immunofluorescence
Intestinal and colonic tissues were prepared as Swiss rolls and sections fixed with 4% paraformaldehyde and β-galactosidase labeling assessed by X-gal staining of frozen sections taken from R26rLacZ mice. Mice were sacrificed at various time points post-tamoxifen and analyzed at the time points specified. We similarly analyzed tissues from R26-mT/mG reporter mice for EGFP-positive cells and their progeny at various time points post-tamoxifen. Further details are outlined in the Supplemental Experimental Procedures. For immunostaining, we performed staining of frozen sections with antibodies according to the methods detailed in the Supplemental Experimental Procedures.

Flow Cytometry
Single-cell suspensions were stained with antibodies and analyzed on FACS Calibur, Aria III (BD) or Gallios (Beckman Coulter). FlowJo software (Ashland) was used for data analysis. Detailed methods and antibodies are described in the Supplemental Experimental Procedures.

In Situ Hybridization
Using a cRNA probe constructed and labeled for *Krt19*, paraformaldehyde-fixed small intestine (SI) and colonic tissues were hybridized with the probe. Detailed methods and antibodies are described in the Supplemental Experimental Procedures.

Statistical Analysis
Statistical analysis was performed with Student's t test or Mann-Whitney when comparing two groups or standard ANOVA analysis with Bonferri correction. Values of * ($p < 0.05$) and ** ($p < 0.01$) were considered statistically significant.

Enteroid In Vitro Cultures
Intestinal or colonic glands units were isolated from mouse as previously described by Bjerknes and Cheng (2006) with some modifications and cultured in the presence of EGF 50 ng/ml (Invitrogen), mNoggin 100 ng/ml (Peprotech), and R-Spondin 1 μg/ml as previously described (Sato et al., 2009). Detailed protocols are described in the Supplemental Experimental Procedures.

SUPPLEMENTAL INFORMATION

Supplemental Information includes Supplemental Experimental Procedures and six figures and can be found with this article online at http://dx.doi.org/10.1016/j.stem.2015.04.013.

REFERENCES

Barker, N., van Es, J.H., Kuipers, J., Kujala, P., van den Born, M., Cozijnsen, M., Haegebarth, A., Korving, J., Begthel, H., Peters, P.J., and Clevers, H. (2007). Identification of stem cells in small intestine and colon by marker gene Lgr5. Nature *449*, 1003–1007.

Barker, N., Ridgway, R.A., van Es, J.H., van de Wetering, M., Begthel, H., van den Born, M., Danenberg, E., Clarke, A.R., Sansom, O.J., and Clevers, H. (2009). Crypt stem cells as the cells-of-origin of intestinal cancer. Nature *457*, 608–611.

Bjerknes, M., and Cheng, H. (2006). Intestinal epithelial stem cells and progenitors. Methods Enzymol. *419*, 337–383.

Brembeck, F.H., Moffett, J., Wang, T.C., and Rustgi, A.K. (2001). The keratin 19 promoter is potent for cell-specific targeting of genes in transgenic mice. Gastroenterology *120*, 1720–1728.

Doetsch, F., Caillé, I., Lim, D.A., García-Verdugo, J.M., and Alvarez-Buylla, A. (1999). Subventricular zone astrocytes are neural stem cells in the adult mammalian brain. Cell *97*, 703–716.

Fearon, E.R., and Vogelstein, B. (1990). A genetic model for colorectal tumorigenesis. Cell *61*, 759–767.

Fre, S., Hannezo, E., Sale, S., Huyghe, M., Lafkas, D., Kissel, H., Louvi, A., Greve, J., Louvard, D., and Artavanis-Tsakonas, S. (2011). Notch lineages and activity in intestinal stem cells determined by a new set of knock-in mice. PLoS ONE *6*, e25785.

Furuyama, K., Kawaguchi, Y., Akiyama, H., Horiguchi, M., Kodama, S., Kuhara, T., Hosokawa, S., Elbahrawy, A., Soeda, T., Koizumi, M., et al. (2011). Continuous cell supply from a Sox9-expressing progenitor zone in adult liver, exocrine pancreas and intestine. Nat. Genet. *43*, 34–41.

Jung, P., Sato, T., Merlos-Suárez, A., Barriga, F.M., Iglesias, M., Rossell, D., Auer, H., Gallardo, M., Blasco, M.A., Sancho, E., et al. (2011). Isolation and in vitro expansion of human colonic stem cells. Nat. Med. *17*, 1225–1227.

Kozar, S., Morrissey, E., Nicholson, A.M., van der Heijden, M., Zecchini, H.I., Kemp, R., Tavaré, S., Vermeulen, L., and Winton, D.J. (2013). Continuous clonal labeling reveals small numbers of functional stem cells in intestinal crypts and adenomas. Cell Stem Cell *13*, 626–633.

Lapouge, G., Youssef, K.K., Vokaer, B., Achouri, Y., Michaux, C., Sotiropoulou, P.A., and Blanpain, C. (2011). Identifying the cellular origin of squamous skin tumors. Proc. Natl. Acad. Sci. USA *108*, 7431–7436.

Li, L., and Clevers, H. (2010). Coexistence of quiescent and active adult stem cells in mammals. Science *327*, 542–545.

May, R., Riehl, T.E., Hunt, C., Sureban, S.M., Anant, S., and Houchen, C.W. (2008). Identification of a novel putative gastrointestinal stem cell and adenoma stem cell marker, doublecortin and CaM kinase-like-1, following radiation injury and in adenomatous polyposis coli/multiple intestinal neoplasia mice. Stem Cells *26*, 630–637.

Means, A.L., Xu, Y., Zhao, A., Ray, K.C., and Gu, G. (2008). A CK19(CreERT) knockin mouse line allows for conditional DNA recombination in epithelial cells in multiple endodermal organs. Genesis *46*, 318–323.

Metcalfe, C., Kljavin, N.M., Ybarra, R., and de Sauvage, F.J. (2014). Lgr5+ stem cells are indispensable for radiation-induced intestinal regeneration. Cell Stem Cell *14*, 149–159.

Moll, R., Franke, W.W., Schiller, D.L., Geiger, B., and Krepler, R. (1982). The catalog of human cytokeratins: patterns of expression in normal epithelia, tumors and cultured cells. Cell *31*, 11–24.

Montgomery, R.K., Carlone, D.L., Richmond, C.A., Farilla, L., Kranendonk, M.E., Henderson, D.E., Baffour-Awuah, N.Y., Ambruzs, D.M., Fogli, L.K., Algra, S., and Breault, D.T. (2011). Mouse telomerase reverse transcriptase (mTert) expression marks slowly cycling intestinal stem cells. Proc. Natl. Acad. Sci. USA *108*, 179–184.

Park, H.S., Goodlad, R.A., and Wright, N.A. (1995). Crypt fission in the small intestine and colon. A mechanism for the emergence of G6PD locus-mutated crypts after treatment with mutagens. Am. J. Pathol. *147*, 1416–1427.

Powell, A.E., Wang, Y., Li, Y., Poulin, E.J., Means, A.L., Washington, M.K., Higginbotham, J.N., Juchheim, A., Prasad, N., Levy, S.E., et al. (2012). The pan-ErbB negative regulator Lrig1 is an intestinal stem cell marker that functions as a tumor suppressor. Cell *149*, 146–158.

Quante, M., Marrache, F., Goldenring, J.R., and Wang, T.C. (2010). TFF2 mRNA transcript expression marks a gland progenitor cell of the gastric oxyntic mucosa. Gastroenterology *139*, 2018–2027.

Ramalingam, S., Daughtridge, G.W., Johnston, M.J., Gracz, A.D., and Magness, S.T. (2012). Distinct levels of Sox9 expression mark colon epithelial stem cells that form colonoids in culture. Am. J. Physiol. Gastrointest. Liver Physiol. *302*, G10–G20.

Ritsma, L., Ellenbroek, S.I., Zomer, A., Snippert, H.J., de Sauvage, F.J., Simons, B.D., Clevers, H., and van Rheenen, J. (2014). Intestinal crypt homeostasis revealed at single-stem-cell level by in vivo live imaging. Nature *507*, 362–365.

Sangiorgi, E., and Capecchi, M.R. (2008). Bmi1 is expressed in vivo in intestinal stem cells. Nat. Genet. *40*, 915–920.

Sato, T., Vries, R.G., Snippert, H.J., van de Wetering, M., Barker, N., Stange, D.E., van Es, J.H., Abo, A., Kujala, P., Peters, P.J., and Clevers, H. (2009). Single Lgr5 stem cells build crypt-villus structures in vitro without a mesenchymal niche. Nature *459*, 262–265.

Seshagiri, S., Stawiski, E.W., Durinck, S., Modrusan, Z., Storm, E.E., Conboy, C.B., Chaudhuri, S., Guan, Y., Janakiraman, V., Jaiswal, B.S., et al. (2012). Recurrent R-spondin fusions in colon cancer. Nature *488*, 660–664.

Stange, D.E., Koo, B.K., Huch, M., Sibbel, G., Basak, O., Lyubimova, A., Kujala, P., Bartfeld, S., Koster, J., Geahlen, J.H., et al. (2013). Differentiated Troy+ chief cells act as reserve stem cells to generate all lineages of the stomach epithelium. Cell *155*, 357–368.

Takeda, N., Jain, R., LeBoeuf, M.R., Wang, Q., Lu, M.M., and Epstein, J.A. (2011). Interconversion between intestinal stem cell populations in distinct niches. Science *334*, 1420–1424.

Tian, H., Biehs, B., Warming, S., Leong, K.G., Rangell, L., Klein, O.D., and de Sauvage, F.J. (2011). A reserve stem cell population in small intestine renders Lgr5-positive cells dispensable. Nature *478*, 255–259.

van Es, J.H., Sato, T., van de Wetering, M., Lyubimova, A., Nee, A.N., Gregorieff, A., Sasaki, N., Zeinstra, L., van den Born, M., Korving, J., et al. (2012). Dll1+ secretory progenitor cells revert to stem cells upon crypt damage. Nat. Cell Biol. *14*, 1099–1104.

Yan, K.S., Chia, L.A., Li, X., Ootani, A., Su, J., Lee, J.Y., Su, N., Luo, Y., Heilshorn, S.C., Amieva, M.R., et al. (2012). The intestinal stem cell markers Bmi1 and Lgr5 identify two functionally distinct populations. Proc. Natl. Acad. Sci. USA *109*, 466–471.